OPEN ACCESS
OPUS AUGSBURG

Universität Augsburg
Universitätsbibliothek

Comparative solvolytic stabilities of copper(II) nanoballs and dinuclear Cu(II) paddle wheel units

Markus Tonigold, Dirk Volkmer

Angaben zur Veröffentlichung / Publication details:

Tonigold, Markus, and Dirk Volkmer. 2010. "Comparative solvolytic stabilities of copper(II) nanoballs and dinuclear Cu(II) paddle wheel units." *Inorganica Chimica Acta* 363 (15): 4220–29. https://doi.org/10.1016/j.ica.2010.06.022.

Nutzungsbedingungen / Terms of use: **CC BY-NC-ND 4.0**

Dieses Dokument wird unter folgenden Bedingungen zur Verfügung gestellt: / This document is made available under these conditions:
CC-BY-NC-ND 4.0: Creative Commons: Namensnennung - Nicht kommerziell - Keine Bearbeitung
Weitere Informationen finden Sie unter: / For more information see:
https://creativecommons.org/licenses/by-nc-nd/4.0/deed.de

Comparative solvolytic stabilities of copper(II) nanoballs and dinuclear Cu(II) paddle wheel units

Markus Tonigold, Dirk Volkmer *

Ulm University, Institute of Inorganic Chemistry 2, Materials and Catalysis, Albert-Einstein-Allee 11, D-89081 Ulm, Germany

1. Introduction

A broad range of existing and future applications for nanometer-sized hollow molecules is currently under discussion in literature: they can serve for instance as nanoreactors, which are a simple mimic of enzymes for a diverse range of thermal and photochemical reactions [1]. Further present applications for (drug) delivery, storage, and separation technology [2] involve molecular recognition, host–guest chemistry and chiral recognition, while long-term goals are focused on the design of new materials with desirable properties and the manufacturing of nanoscale devices and molecular machinery [3,4].

Tracking these aims, metal-organic polyhedra (MOPs, also named nanoballs, nanocontainers or nanocages) [4–7], have come to the foreground in the last few years, in addition to the well-established organic molecular containers [8]. MOPs are built through the interconnection of metal ions or clusters with simple, polyfunctional organic ligands (so-called linkers, mostly containing nitrogen or carboxylate groups as complex builders). One way to obtain nanoballs in high yield is to interconnect copper(II) paddle wheel complexes at a 120° angle with the bifunctional ligand benzene-1,3-dicarboxylate (bdc) or its derivatives [4–7]. By changing the substituent *R* in the 5-position of bdc, nanoballs which are highly soluble in polar solvents (e.g. alcohols or N,N-dimethylformamide (DMF) for *R* = OH [5a], DMF or dimethyl sulfoxide (DMSO) for *R* = OC_2H_5OH [6]), or in nonpolar solvents (e.g. toluene, dichloromethane or THF for *R* = $OC_{12}H_{25}$ [5d]) are obtained.

Especially for the applications mentioned above, knowledge about *kinetic* and *thermodynamic* stability of these molecular containers is crucial. Studies on the *disassembly kinetics* of smaller supramolecular architectures (such as helices [9] and organic self-assemblies) [10] have been intensively performed, but to date only a few studies focus on the *kinetic stability* of larger, nanometer-sized metal-organic polyhedra [6,7]. To the best of our knowledge, no studies concerning the *thermodynamic stability* of metal-organic polyhedra or similar compounds have been carried out in detail yet.

We have already shown earlier that nanoballs based on interconnected copper(II) paddle wheels are *kinetically* far more stable in solvents like DMF or DMSO than the (kinetically labile) dinuclear copper(II) paddle wheel complexes such as copper acetate or benzoate, which is presumably due to their more rigid structure (as shown for *R* = OC_2H_5OH in 5-position of bdc by spectrophotometry) [6].

Since the *kinetic stability* compared to simple paddle wheel units is increased due to the structural features of the nanoball,

* Corresponding author. Tel.: +49 (0)731 50 23921; fax: +49 (0)731 50 23039.
E-mail address: dirk.volkmer@uni-ulm.de (D. Volkmer).

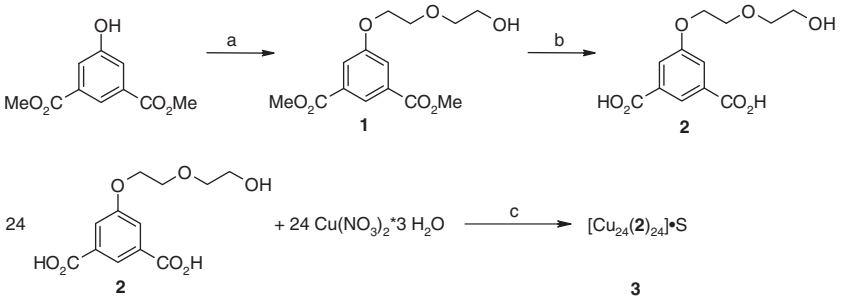

Scheme 1. Synthetic route for linker **2** and nanoball **3**. a: KI, K_2CO_3, CH_3CN, reflux, 24 h; b: (1) KOH, EtOH/H_2O (1:1), reflux, 6 h (2) HCl; c: 2 equivalents 2,6-dimethylpyridine, methanol, room temperature, 1 min. S: solvent molecules.

the question about the influence on the *thermodynamic stability* arises. Dinuclear copper(II) carboxylates (to which we refer as a reference standard) are remarkably dissociated in aqueous solution [11], whereas the dissociation is strongly decreased for less polar solvents [12]. For hydroxylated nanoballs (R = OH in 5-position of bdc) in methanol solution, spectroscopic studies even showed no detectable dissociation at all [13], qualitatively showing the increased thermodynamic stability above the underlying dinuclear copper(II) carboxylates. Since the thermodynamic stability of these nanoballs seems to be most interesting for aqueous solutions, we thus prepared a new nanoball based on a bis(ethylene glycol)-functionalized linker which is soluble in H_2O:DMF (1:1) to quantify the thermodynamic stability, as existing functionalised nanoballs [5,6] in our hands showed poor solubility in aqueous solvents.

Whether the thermodynamic stability is increased, or even decreased, depends on the cooperativity of the system. Cooperativity [14] arises from the interplay of two or more interactions, so that the system as a whole behaves differently from expectations based on the properties of the individual interactions acting in isolation. Coupling of interactions can lead to positive or negative cooperativity, depending on whether one interaction favours or disfavours another. Positive cooperativity implies a low concentration of intermediates. Positive cooperativity leads to a low peak concentration of intermediates and a sharp transition from unbound to bound. In other words, as the system approaches the limit of strong positive cooperativity, only the extreme states are significantly populated. Cooperativity exhibited in the folding of proteins and supramolecular self-assemblies is driven by the difference in strength between the intermolecular and intramolecular interactions, and is a consequence of the molecular architecture. This phenomenon gives rise to the chelate effect [15], and is thus also called chelate cooperativity.

Already small organic assemblies [16], inorganic cylindrical architectures [17] or double helicates [9a–c] show increased thermodynamic stabilities due to positive cooperative effects, and an even more pronounced influence on the nanoball built from 48 subunits might be expected.

Furthermore, the formation of insoluble coordination polymers is always given as a possible concurrence to the dissociation of a supramolecular self-assembly into its constituents: by linking copper(II) paddle wheel complexes with functionalised benzene-1,3-dicarboxylate (bdc), two- or three-dimensional networks [18,19] might be obtained instead of nanoballs. Which of these competing products occurs depends on the formation of kinetic products, the concentrations of the educts, the ligand-to-metal ratio, pH, solvent effects, template molecules which direct the course of the assembly, and temperature [1,20–22]. Among these, the concentrations and the ligand-to-metal ratio are the most crucial for the self-assembly of cyclic or spherical self-assemblies.

2. Results and discussion

The linker 5-(2-(2-hydroxyethoxy)ethoxy)benzene-1,3-dicarboxylic acid **2** was synthesized from dimethyl-5-hydroxybenzene-1,3-dicarboxylate and 2-(2-chloroethoxy)ethanol to give the intermediate **1**, which was subsequently saponified and afterwards protonated to yield **2** in an overall yield of 77% (Scheme 1).

From an equimolar solution of **2** and $Cu(NO_3)_2{\cdot}3H_2O$ in methanol, the nanoball $[Cu_{24}(C_{12}H_{12}O_7)_{24}]{\cdot}24MeOH$ **3** immediately precipitates upon adding two equivalents of 2,6-dimethylpyridine.[1] Recrystallisation from dimethylsulfoxide (DMSO) and butanol afforded **3b** as green crystals suitable for single crystal X-ray diffraction studies.

To evaluate the dissociation stability of **3**, it is necessary to facilitate the dissociation of the complexes by adding an acid, since the dissociation of the nanoball is kinetically hindered. For this purpose, it might seem reasonable to add the diprotonated ligand **2** to a solution of the nanoball **3**. Consequently, a closed spherical structure starts to compete with open polymeric structures if the ratio in solution after dissociation mismatches the stochiometry of the spherical structure: compared to open polymeric structures, an increased number of bonds between the constituents is possible in a cyclic or spherical arrangement, and will be favoured from the enthalpic point of view (since the donor and acceptor sites at each end of the polymer will always remain uncoordinated). However, when the ligand-to-metal ratio in solution mismatches the stochiometry of the cyclic or spherical supramolecular assembly, the enthalpic advantage diminishes due to the present excess of donor or acceptor sites [1,20–22]. Accordingly, when the nanoball **3** is dissolved in H_2O:DMF (1:1) together with three equivalents of the ligand **2** per copper atom, the nanoball slowly transforms throughout several weeks into single crystals of the three-dimensional network $[Cu(C_{12}H_{12}O_7)]{\cdot}0.5\ H_2O{\cdot}0.5$ DMF **4**. This course from least stable to more stable (as well as less dense to more dense) polymorph of $Cu(C_{12}H_{12}O_7)$ follows the classical Ostwald–Volmer rule [23]. Only slow dissociation and no transformation is observed after the addition of acetic acid, emphasising the strong influence of the ligand-to-metal ratio for the stability of the nanoball over open polymeric structures. Therefore, the dissociation constant of **3** can be determined after the addition of acetic acid (see below).

Noteworthly, no transformation of **3** into a three-dimensional network is observed for solutions in anhydrous DMF or DMSO. These solutions have remained unchanged for up till now more than 12 months – even when up to 500 equivalents of the diacid ligand **2** per copper atom are present in these solutions. These results show, in analogy to the strongly increased stability against

[1] The exact number and kind of coordinated solvent molecules is difficult to determine for this class of substances [4a] and was chosen according to elemental and thermogravimetric analyses.

dissociation of simple dinuclear copper(II) paddle wheel complexes, that the nanoball **3** seems to be virtually undissociated in organic solvents (even at high concentrations of H_2L). The structure remains intact and no transformation is observed even at very high ligand-to-metal ratios (500:1).

For **3**, thermogravimetric analysis (TGA) shows a negligible weight loss of 5.1% in the temperature range of 30–269 °C (expected: 8.8% for complete loss of methanol). Further weight loss of 67.4% occurs from 269 to 400 °C which is ascribed to the decomposition of the nanoball **3**. These results indicate a thermodynamic stability against decomposition similar to related compounds [5b] up to at least 269 °C. For **4,** a weight loss of 11.6% is observed in the temperature range of 30–260 °C (expected: 13.6% for complete loss of DMF and water). Further weight loss of 66% occurs from 260 to 600 °C due to decomposition.

2.1. X-ray structure analyses

To avoid rapid loss of occluded solvent molecules, crystals of **3b** and **4** were directly covered with mineral oil after removing them from the mother liquor. Crystals of compound **3b** were found to be completely stable if stored in the mother liquor. However, upon exposing them to air, crystallinity is lost within minutes, leading to an uncertain number of occluded solvent molecules, which is common for metal-organic structures with open porosity [4a,5b]. Whereas problems of crystal aging could be minimised experimentally, some unavoidable problems in refining the structure of **3b** arose from the fact that the solvent molecules occluded in the crystal lattice as well as the 2-(2-hydroxyethoxy)ethoxy substituent of the linker are largely disordered. These disordered groups had to be refined as rigid fragments using restraints with appropriate atomic coordinates taken from literature [24]. The solvent atoms coordinated to the copper atoms could be refined as DMSO, water and methanol. Due to their high disorder we were not able to determine the exact amount and identity of the solvent molecules included in the voids of **3b**, thus PLATON/SQUEEZE [25] was used to correct the data for the presence of the disordered solvent. A potential solvent volume of 22 437 $Å^3$ containing 7848 electrons was found, corresponding to an electron density of 0.350 e $Å^{-3}$ (expected for *n*-butanol: 0.489 e $Å^{-3}$, for DMSO: 0.664 e $Å^{-3}$ calculated from the molar mass and density at room temperature), whose contribution was removed by the PLATON/SQUEEZE program [25]. Beside these problems, the general connectivity of the rigid part of nanoball **3b** is proven, and the structure is further confirmed by SAXS measurements in solution (see below).

3b has an outer dimension (measured from opposite groups at the periphery) of 3.2 nm and consists of 12 Cu paddle wheel units interconnected via 24 linkers (Fig. 1a). The internal cavity has a diameter of 1.6 nm without terminal ligands, and the 12 paddle wheel units form a cuboctahedron (Fig. 1b) composed of linked vertices of squares (Fig. 1c).

Neighboured paddle wheel units in **3b** are 1.0 nm apart from each other (measured from the centres of the dinuclear units) and represent the vertices of triangular and square apertures. These openings have widths of about 0.6 and 1.2 nm, respectively (height of the triangular and diagonal of the square aperture, taking into account the Van-der-Waals radii) [26]. The dimensions of the windows as well as the distances and angles within **3b** are statistically identical to those observed in structurally related nanoballs featuring a $\{Cu_{24}(bdc)_{24}\}$ core [5,6].

The coordination polymer **4** is formed solely from square windows (Fig. 2) by bridging the paddle wheel units via the carboxylate groups into two-dimensional layers along the *a*- and *b*-axis. These layers are piled along the *c*-axis, providing a one-dimensional pore system. Half of the 2-(2-hydroxyethoxy)ethoxy side chains in one two-dimensional layer coordinate with their hydroxy

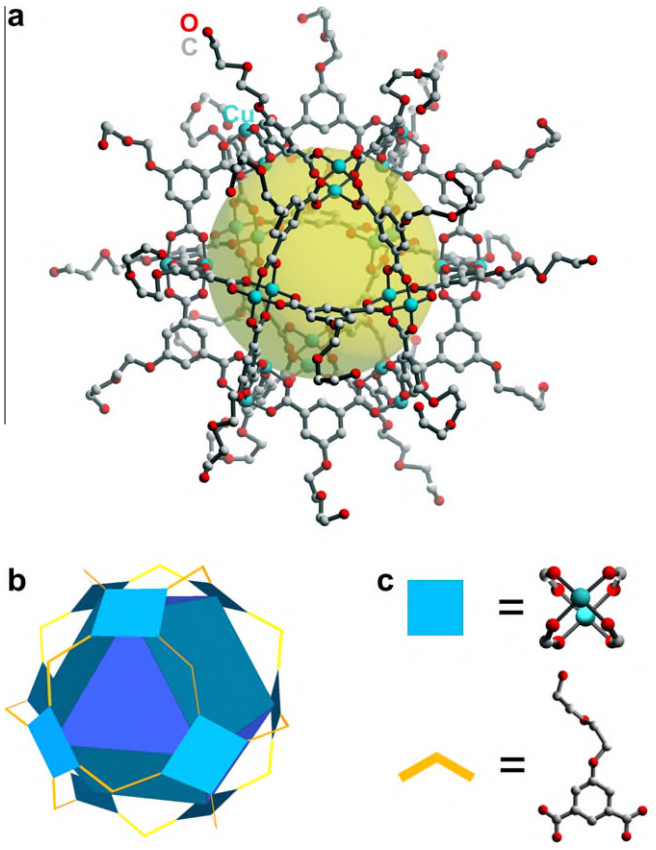

Fig. 1. (a) Ball-and-stick representation of the X-ray single-crystal structure of **3b**. Cu, blue; O, red; C, grey. Hydrogen atoms and coordinated and guest solvent molecules are omitted for clarity. The yellow sphere represents the internal cavity. (b) Schematic representation of **3b** as a cuboctahedron (showing the positions of the triangular and square apertures) comprised from (c) $Cu_2(CO_2)_4$ paddle-wheel (squares) linked at an 120° angle by **2**. (For interpretation of the references to colour in this figure legend, the reader is referred to the web version of this article.)

groups to the copper atoms of the neighboured layer, thus interconnecting the two-dimensional grids to a three-dimensional network (Fig. 3). Two different kind of windows are alternatingly present: one in which all linker molecules are facing the same direction, and another where only the pairs of opposing ligands are facing the same direction (and the other pair the opposite direction), a MOF structural motif which is already known in literature [18].

Compared to the two-dimensional layers described in literature to date, which are not covalently connected with each other, the extensive 2-(2-hydroxyethoxy)ethoxy side chains in **4** are long enough to coordinate with their hydroxy groups to the copper atoms of the neighboured layer, thus interconnecting the two-dimensional grids to a three-dimensional network (Fig. 3).

Only half of the side chains are coordinated to the copper atoms of the next layer: the side chains of the ligands which connect the copper atoms parallel to the *a*-axis bind to the next layer, whereas the side chains of the ligands which connect the copper atoms parallel to the *b*-axis protrude into the voids of the crystal. Torsional strain that has to be overcome seems to be the reason that not all side chains are coordinated. The ligands which bridge the paddle wheel units parallel to the *a*-axis have torsion angles between the carboxylate groups and the benzene ring of 14.6° and 18.9°, whereas the ones bridging parallel to the *b*-axis have torsion angles of only 4.1° and 6.9°. As a result, the ligands bridging along the *a*-axis are more bent towards the *c*-axis (see Fig. 2), and are therefore in enough short distance to coordinate to the next layer (the dis-

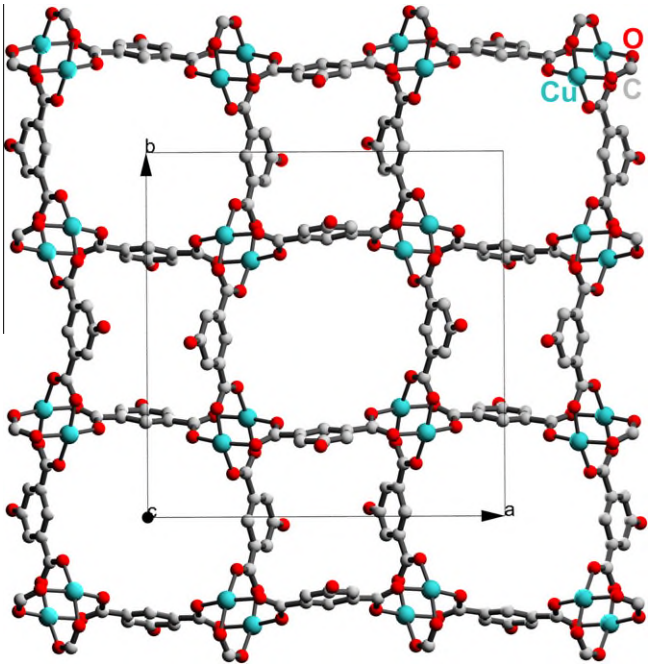

Fig. 2. (a) View along the *c*-axis of a ball-and-stick representation of the X-ray single-crystal structure of **4**. Cu, blue; O, red; C, grey. Hydrogen atoms, coordinated and guest solvent molecules and bisethyleneglycol side chains are omitted for clarity. (For interpretation of the references to colour in this figure legend, the reader is referred to the web version of this article.)

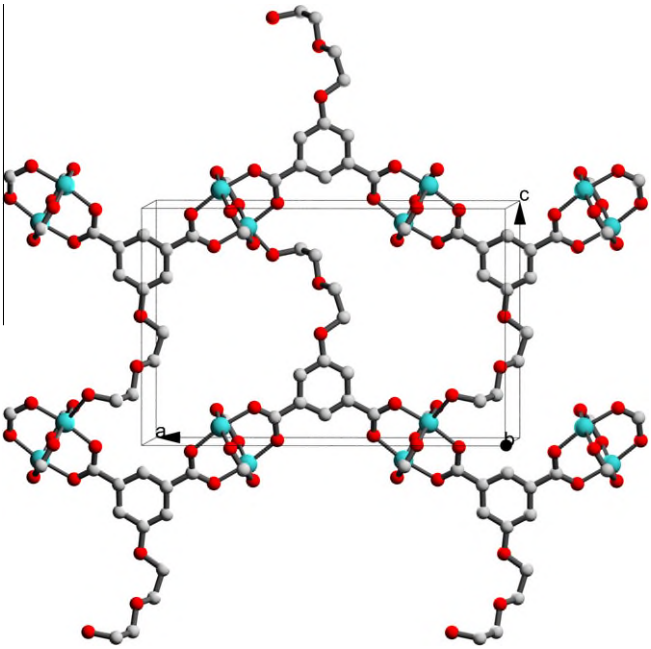

Fig. 3. (a) View along the *b*-axis of a ball-and-stick representation of the X-ray single-crystal structure of **4**. Cu, blue; O, red; C, grey. Hydrogen atoms and coordinated and guest solvent molecules are omitted for clarity. (For interpretation of the references to colour in this figure legend, the reader is referred to the web version of this article.)

tance between the oxygen atom in the 5-position of bdc to the closest copper atom in the next layer is 6.7 Å for the bent ligands, whereas it is 8.0 Å for the ones with uncoordinated side chains).

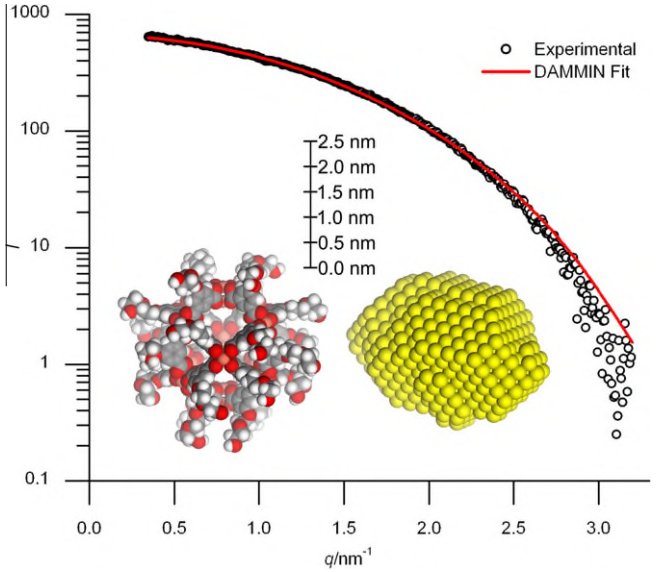

Fig. 4. Main plot: SAXS intensity (I) vs. momentum transfer (q = 0.2–3.2 nm) for a solution of **3** in DMF (18 g/L). The symbols and the solid line correspond to the experimental data points and the numerical fit using GNOM/DAMMIN simulated annealing (χ = 2.941), respectively. Inset: spacefilling model of **3** and bead model from low-resolution particle shape reconstruction for **3** obtained by the GNOM/DAMMIN fit.

2.2. Small-angle X-ray scattering (SAXS)

SAXS measurements, which provide the shape and internal structure of particles in solutions [27], were conducted to confirm that the structural features of **3** persist in solution. The logarithmic plot of SAXS intensity (I) versus momentum transfer (q) for **3** is shown in Fig. 4 together with the numerical fit to the SAXS data evaluating the shape in solution. The representative reconstruction of the low resolution three-dimensional particle shape was provided by simulated annealing using the GNOM/DAMMIN software packages [28,29] and matches the shape and dimensions of **3** well (see Fig. 4).

The radius of gyration (R_g) obtained from the SAXS data for **3** is 1.1 nm, in excellent agreement with the expected shape: due to the crystal structure analysis, the distances of the interior and exterior copper ions from the centre of the nanoballs **3** are 0.8 and 1.1 nm, respectively. The maximal distance from the centre to the periphery is 1.9 nm.

Principally, bead models derived from experimental SAXS data show an effective spatial resolution of approximately 0.5 nm for molecules with radii of gyration below 1.5 nm [30].

Using the X-ray single-crystal structure data of **3b**, we additionally calculated its hypothetical scattering intensities with the program CRYSOL [31], which matches the observed experimental intensities well (Fig. S2, Supplementary Material).

2.3. Thermodynamic stability

To compare the thermodynamic stability of the nanoball **3** with simple dinuclear copper(II) paddle wheel complexes, dilution experiments were performed, measuring the absorbances for different initial concentrations of the complexes. The ionic strength was fixed at 0.5 M using KNO_3. Lower initial concentrations (Cu_{tot}) lead to an increased dissociation, which results in decreased molar absorbances (Fig. 5), since the typical band I of copper(II) paddle wheel complexes [32] (maximum absorption at 710 and 730 nm in H_2O and DMF:H_2O 1:1, respectively) disappears to yield isolated and fully solvated copper(II) ions (maximum absorption at 800 and

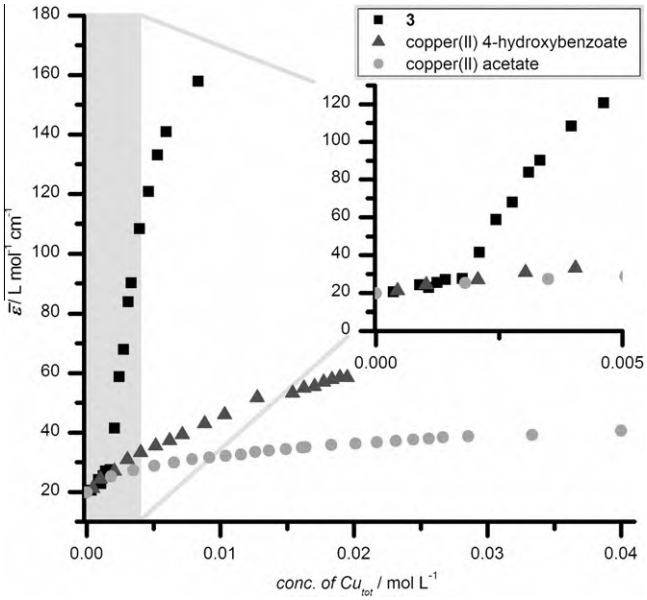

Fig. 5. Apparent molar absorbances at 770 nm for copper(II) acetate (●), copper(II) 4-hydroxybenzoate (▲) and **3** (■) in H_2O:DMF 1:1 vs. the total copper concentration Cu_{tot}.

$$\mathrm{Cu(O_2CR)_2} \rightleftharpoons \underset{\textbf{1:1}}{\mathrm{Cu(O_2CR)^+ + (O_2CR)^-}} \rightleftharpoons \underset{\textbf{2:1}}{\mathrm{Cu^{2+} + 2\,(O_2CR)^-}}$$

$\mathbf{R} = \bullet CH_3$ or $\bullet C_6H_5OH$

$$\mathrm{Cu(O_2CR)_2} \rightleftharpoons \mathrm{Cu(O_2CR)^+ + (O_2CR)^-} \qquad K_1$$
$$\mathrm{Cu(O_2CR)^+} \rightleftharpoons \mathrm{Cu^{2+} + (O_2CR)^-} \qquad K_2$$

Scheme 2. Two-step dissociation equilibria for simple copper(II) carboxylates.

815 nm in H_2O and DMF:H_2O 1:1, respectively). At very low concentrations, the molar absorbances approach the values for copper(II) ions in solution, whereas at high concentrations, they approximate the values of the dinuclear complexes or the nanoball, respectively.

Already these courses of the molar absorbances versus the initial concentrations (Cu_{tot}) of the complexes reveal an obviously different dissociation behaviour for the nanoball **3** compared to the simple dinuclear paddle wheel complexes. The nanoball shows a much steeper increase in absorbance (equivalent to a sharp free-to-bound transition over a narrow concentration range), and furthermore a sigmoidal (S-shaped) course of absorbances in contrary to the dinuclear complexes.

2.4. Thermodynamic stability of simple paddle wheel complexes in aqueous solvents

To compare the thermodynamic stability of the nanoball **3** with simple dinuclear copper(II) paddle wheel complexes, we first evaluated the dissociation constants of copper(II) acetate and copper(II) 4-hydroxybenzoate (which is more comparable to the aromatic dicarboxylic acid **2**) via spectrophotometry according to the procedure described in literature.[2]

In water, copper(II) acetate behaves essentially as a 1:1 electrolyte at concentrations greater than about 0.1 M, whereas at lower concentrations it dissociates as a 2:1 electrolyte, according to the two equilibria shown in Scheme 2.

To facilitate the dissociation of the complexes as described in the original literature [11a] for copper(II) acetate in water, 0.140 mol/L acetic acid or 4-hydroxybenzoic acid, respectively, were added prior to the measurements. The obtained course of molar absorbances ($\bar{\varepsilon}$, calculated for Cu_{tot}, the total concentration of copper atoms in solution) versus total copper concentrations Cu_{tot} was evaluated at 770 (Fig. 5) and 680 nm according to Eq. (1) (derivation as described in Supplementary Material) [11a],

$$\bar{\varepsilon} = \frac{\varepsilon_{Cu(O_2CR)_2}[Cu(O_2CR)_2] + \varepsilon_{Cu(O_2CR)^+}[Cu(O_2CR)^+] + \varepsilon_{Cu^{2+}}[Cu^{2+}]}{Cu_{tot}} \quad (1)$$

simplifying the dinuclear complexes as $[Cu(O_2CR)_2]$, giving

$$Cu_{tot} = [Cu(O_2CR)_2]_0 = [Cu(O_2CR)_2] + [Cu(O_2CR)^+] + [Cu^{2+}] \quad (2)$$

The formulation $Cu(O_2CR)_2$ (and not $Cu_2(O_2CR)_4$) was chosen according to literature, since the experimental data can thus be fit to a much simpler model (containing only two dissociation steps and three compounds, see Supplementary Material for more details). The fact that this simpler model is able to completely describe the experimental course of absorbances justifies the avoidance of a more complicated model. Furthermore, only the extinction coefficients for the dincluear complexes and Cu^{2+} are directly available experimentally, whereas the extinction coefficients of the intermediate species have to be determined during the data fitting. Therefore, the extinction coefficients for the additional intermediate species and the respective equilibria constants (which would be introduced using a more complex model for the dissociation of $[Cu_2(O_2CR)_4]$) would not be determined as accurately as the constants from the model described in Eq. (1) via spectrophotometric measurements. As described [11a], the molar absorbance $\varepsilon_{Cu^{2+}}$ in Eq. (1) is equal to the molar absorbance coefficient of copper(II), whereas the molar absorption of the copper(II) carboxylates ($\varepsilon_{Cu(O_2CR)_2}$) was obtained by adding sodium acetate or sodium 4-hydroxybenzoate to shift the equilibrium towards $Cu(O_2CR)_2$ at high concentrations. $\varepsilon_{Cu(O_2CR)^+}$ as well as finally K_1 and K_2 were obtained by fitting the theoretical course of the molar absorbances to the experimental data at 770 and 680 nm (see Supplementary Material for details). Since **3** as well as copper(II) 4-hydroxybenzoate show poor solubility in pure water, we examined the complex dissociation constants K_1 and K_2 for copper(II) 4-hydroxybenzoate in H_2O:DMF 1:1, and for copper(II) acetate both in water and in H_2O:DMF 1:1 (Table 1).

Both dissociation constants for copper(II) acetate are approximately halved when switching from H_2O to H_2O:DMF 1:1, which displays a negligible increase in stability when compared to the more drastic changes when water is completely replaced by an organic solvent [12,13]. Compared to copper(II) acetate, copper(II) 4-hydroxybenzoate shows similar stability against dissociation (with a slightly decreased first dissociation constant K_1 and a slightly increased second dissociation constant K_2).

2.5. Thermodynamic stability of nanoballs in aqueous solvents

To investigate the thermodynamic stability of the nanoball, solutions of **3** in H_2O:DMF 1:1 with different initial concentrations were prepared. To facilitate the dissociation of the complexes, two

Table 1
Stepwise complex dissociation constants (mol L^{-1}) and overall dissociation constants (pK = −log K_1·K_2) for the simple dinuclear complexes copper(II) acetate and copper(II) 4-hydroxybenzoate.

R	Solvent	K_1	K_2	pK
CH_3	H_2O	0.11(3)	0.016(4)	2.8(5)
CH_3	H_2O:DMF 1:1	0.052(14)	0.0085(22)	3.4(5)
HOC_6H_4	H_2O:DMF 1:1	0.023(6)	0.017(4)	3.4(5)

[2] The dissociation constants K_1 and K_2 of copper (II) acetate in water
$Cu(OAc)_2 \rightleftharpoons Cu(OAc)^+ + OAc^-$ K_1,
$Cu(OAc)^+ \rightleftharpoons Cu^{2+} + OAc^-$ K_2
were earlier determined to be −log K_1 = 0.9–1.0 and −log K_2 = 1.6–2.4 (temperature range 15–35 °C; ionic strength range 0–3.0) [11].

equivalents of acetic acid per copper(II) atom in the solution were added. The absorbances slowly decreased after the addition of acetic acid and reached their final value after 2–3 months (as monitored by spectrophotometry). No effect on the finally obtained absorbances (and thus the equilibrium concentrations) was observed for different concentrations of acetic acid per copper(II) atom (until up to four equivalents), ensuring that acetic acid is only acting as a catalyst for the dissociation. After 6 months, the molar absorbances for the different initial concentrations of the nanoball **3** were measured. The recorded molar absorbances per copper atom versus the initial concentrations of **3** were evaluated at 770 (Fig. 5) and 680 nm, showing an obviously different course of absorbances compared to simple copper(II) carboxylates.

Below Cu_{tot} = 1.7 mmol/L, the molar absorbances which we obtained show only a slight increase with the concentration and nearly equal the molar absorbances of copper(II). This indicates that below 1.7 mmol (which can therefore be seen as a lower critical self-assembly concentration) only copper(II) and presumably small fragments of the nanoball are present in solution. Above this concentration, a distinct increase in molar absorbance is observed, which converges at high concentrations to the molar absorbance of the nanoball. This behaviour resembles supramolecular micelle formation and the behaviour at the critical micelle concentration (cmc) [33] and is in agreement with the theoretical course of concentrations for supramolecular assemblies around the critical self-assembly concentration [22]. In analogy to the dissociation equilibria of the simple dinuclear copper(II) paddle wheel complexes, the experimental data fit a dissociation model in which the nanoball fragmentates into simple species ("CuL"), which is further on in equilibrium with copper(II) ions and free deprotonated ligand **2** in solution (Scheme 3). Although the structure of the nanoball is quite complicated, and principally there could be many intermediate products involved, the simple theoretical model is suitable to fit the experimental data, showing that the concentrations of possible intermediates are too low to significantly contribute to the final absorbances.

The obtained course of molar absorbances versus concentrations was evaluated at 770 and 680 nm according to Eq. (3) (regarding the apparent molar absorbances per copper atom),

$$\bar{\varepsilon} = \frac{12 \cdot \varepsilon_{Cu_{12}L_{12}}[Cu_{12}L_{12}] + \varepsilon_{CuL}[CuL] + \varepsilon_{Cu^{2+}}[Cu^{2+}]}{Cu_{tot}} \quad (3)$$

thus simplifying the nanoball as $[Cu_{12}L_{12}]$, giving

$$Cu_{tot} = 12 \cdot [Cu_{12}L_{12}] + [CuL] + [Cu^{2+}] \quad (4)$$

Without the addition of acid, the nanoball **3** is kinetically inert in solution, thus its molar absorption $\varepsilon_{Cu_{12}L_{12}}$ was simply obtained from solutions of **3** in H_2O:DMF 1:1. ε_{CuL} as well as finally $pK_1 = 32.5 \pm 0.41$ and $pK_2 = 2.74 \pm 0.25$ were obtained by fitting the theoretical course of the molar absorbances to the experimental data at 770 and 680 nm (see Supplementary Material). The overall dissociation constant (dissociation of the nanoball into Cu^{2+} and ligand L^{2-}) is $pK = p(K_1 \cdot 12K_2) = 65.4$.

A direct comparison of the overall dissociation constant of the nanoball ($K = 10^{-65.4}$ mol^{23} L^{-23}) with simple dinuclear paddle wheel complexes ($K = 10^{-3.4}$ mol^2 L^{-2} for both) is difficult due to the different units of these stability constants. However, a comparison is possible for the stepwise dissociation constants K_1 and K_2 (when K_1 for the nanoball is divided into appropriate equal dissociation steps). Thus, the value of $K_1 = 10^{-32.5}$ mol^{11}/L^{11} can be thought to be theoretically composed of 11 distinct steps, in each of which one dinuclear unit is released from the nanoball (Eq. (5)).

$$\begin{aligned} Cu_{12}L_{12} &\rightleftharpoons Cu_{11}L_{11} + CuL \quad K_{1,1} \\ Cu_{11}L_{11} &\rightleftharpoons Cu_{10}L_{10} + CuL \quad K_{1,2} \\ Cu_{10}L_{10} &\rightleftharpoons Cu_9L_9 + CuL \quad K_{1,3} \\ &\cdots \\ Cu_2L_2 &\rightleftharpoons 2CuL \quad K_{1,11} \end{aligned} \quad (5)$$

Since each of these steps involve the disconnection of at least one carboxylic group from a copper paddle wheel complex of the nanoball, each release step of CuL can be generally compared to the release of $(O_2CR)^-$ from a simple, dinuclear paddle wheel complex. Thus K_1 from the dissociation of these simple complexes is comparable to each of the distinct dissociation steps ($K_{1,1}$, $K_{1,2}$, and so on) of the nanoball. Simply assuming that all dissociation constants of these distinct steps are equal provides us an average value for each distinct dissociation step of $K_{1,1} = K_{1,2} = K_{1,3} = \ldots = K_{1,11} = \sqrt[11]{K_1} = 0.0011$ mol/L, which is 20–50 times less than K_1 for the simple dinuclear paddle wheel complexes (0.051 and 0.023 mol/L for copper(II) acetate and 4-hydroxybenzoate, respectively). A similar increase in stability is observed when regarding the K_2 value (0.0018 mol/L for the nanoball, compared to 0.0085 and 0.017 mol/L for copper(II) acetate and 4-hydroxybenzoate, respectively).

To illustrate the increased stability of the nanoball compared to the comprising dinuclear complexes, we can exemplarily calculate that at a total concentration $Cu_{tot} = L^{2-} = 0.055$ mol L^{-1} of copper(II) ions present in solution (the sum of all copper atoms present in any species), 95% of copper(II) ions can be found in the nanoball, whereas under corresponding conditions only 51% or 39% of totally present copper(II) ions can be found in binuclear copper(II) acetate or 4-hydroxybenzoate, respectively, showing qualitatively the increased stability of the nanoball over simple binuclear complexes. Moreover, 50% of the copper(II) ions still remain in the nanoball at a concentration of $Cu_{tot} = 0.0046$ mol L^{-1}, whereas only 8% or 5% of totally present copper(II) ions can be found in binuclear copper(II) acetate or 4-hydroxybenzoate, respectively.

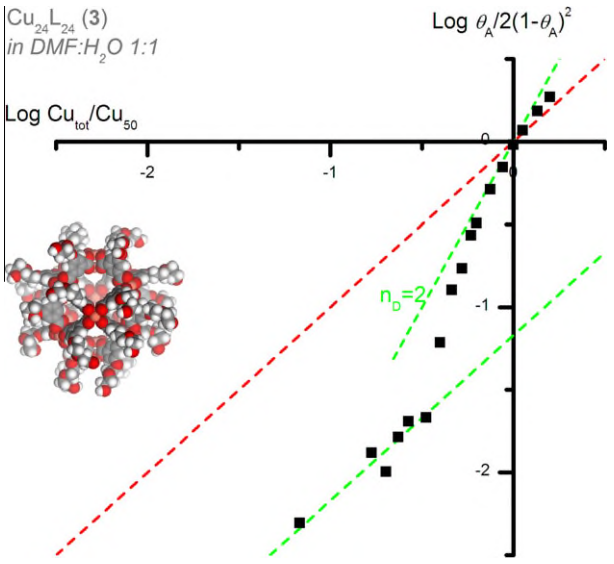

Fig. 6. Modified Hill plot for the Nanoball **3** in DMF:H_2O 1:1. The red line passes the origin with a slope of one and is given as a guide for the eye (displaying the behaviour of a system without cooperativity). The *x*-axis was scaled relative to Cu_{50}, the concentration at 50% site occupancy. (For interpretation of the references to colour in this figure legend, the reader is referred to the web version of this article.)

$$\begin{aligned} Cu_{12}L_{12} &\rightleftharpoons 12\ CuL \quad K_1 \\ CuL &\rightleftharpoons Cu^{2+} + L^{2-} \quad K_2 \end{aligned}$$

Scheme 3. Two-step dissociation equilibria for the nanoball **3**.

Positive cooperativity [14] is the underlying reason for the increased stability of the supramolecular nanoball **3** against dissociation compared to simple dinuclear paddle wheel complexes. The sigmoidal course, which is already visible from the course of absorbances (Fig. 5), is also represented in the binding isotherms of **3** (Supplementary Material), and a modified Hill plot[3] reveals a value of $n_D \approx 2$ and furthermore shows all indications of positive cooperativity for the supramolecular nanoball (Fig. 6). In contrary, the simple dinuclear copper(II) paddle wheel complexes show no signs of cooperativity (see Supplementary Material for an extended discussion).

A further simple explanation of the enhanced dissociation stability of the nanoball **3** in comparison with simple copper(II) paddle wheel complexes is given by the chelate effect (the underlying driving force for positive cooperativity in this kind of supramolecular assembly). The chelate effect in general is predominantly due to a gain in translational entropy (whereas the contribution of ring, conformational or steric strain energies or preorganisation as in macrocycles or cryptants are usually comparably small) [34]. Since the base of the chelate effect is predominantly a result of changes in translational entropy, chelation principally causes a similar decrease of overall dissociation constants: A general decrease of pK by a value of 1.5–4 is observed per exchange of two monodentated with one comparable bidentate ligand [34]. Applying this general observation to the case of the nanoball, we have one molecule which is comprised of 12 dinuclear copper(II) paddle wheel subunits (bridged by 24 bifunctional ligand molecules), which has to be compared with 12 simple dinuclear copper(II) paddle wheel complexes (possessing 48 monofunctional carboxylic ligands in total). When comparing the nanoball with the comprising subunits, we therefore replace 48 monofunctional ligands with 24 bifunctional ligands, leading to an expected increase of the overall dissociation constant $-\log K$ by a value between 36 and 96 (equal to 24 times the effect for exchanging two monodentated with one comparable bidentate ligand). The overall dissociation constants of the simple dinuclear paddle wheel complexes is pK = 3.4 for both copper(II) acetate and copper(II) 4-hydroxybenzoate in DMF:H_2O 1:1, respectively. Therefore, an overall dissociation constant for the nanoball between 40 and 100 would be expected. Indeed, the overall dissociation constant of the nanoball (pK = 65.4) lies in the expected range for an increased stability due to the classical chelate effect.

3. Conclusions

We have presented the synthesis of a new, highly soluble hydroxy-functionalised nanoball which is based on the fundamental copper(II) nanoball coordination unit previously reported by Zaworotko and co-workers [5c]. Nanoballs are thermodynamically more stable than simple dinuclear copper(II) paddle wheel complexes such as copper acetate or benzoate due to the chelate effect (or, in other words, positive chelate cooperativity). The increased stability compared to simple dinuclear copper(II) complexes represents a promising perspective for using water-soluble nanoballs for technological applications or in antifouling coatings in the future. Furthermore, it must be emphasised that the dissociation is only observed in aqueous solvents, whereas in organic solvents no indications for dissociation can be detected.

[3] The slope at the origin of this modified Hill plot, n_D, is a measure for the cooperativity of the system, generally indicating *positive cooperativity* for $n_D > 1$. For *large cyclic oligomers* (such as our nanoball), the modified Hill plot starts parallel to the reference line for low concentrations, and deviates over the concentration range where the macrocycle is the most stable species (with a slope $n_D > 1$ at the origin) in the case of strong *positive cooperativity*.

However, despite the highly increased overall dissociation constant, the metal-to-ligand ratio plays a crucial role: when (by adding additional diprotonated ligand) the ratio in solution mismatches the stochiometry of the nanoball, slow transformation into a three-dimensional network is observed.

In a wider context, these results are also capable of explaining the thermodynamic stability of the related class of metal-organic frameworks (MOFs) [35]. Also here, the stability of these three-dimensional supramolecular architectures should exceed the stability of the underlying simple complexes from the secondary building units. In this light, the results give a promising outlook for the future design of stable and catalytically active MOFs, possibly remaining framework topography and preventing metal leaching even when the simple underlying complexes are less stable.

4. Experimental section

4.1. Materials and methods

Melting points (uncorrected): Büchi Melting Point B-540 apparatus. Infrared spectra: Bruker FTIR IFS 113v spectrometer; KBr pellets. UV–Vis spectra: J&M TIDAS. NMR spectroscopy: Bruker DRX 400; data given as ppm; spectra referenced to the residual solvent peak. CI mass spectra: Finnigan MAT, SSQ 7000 mass spectrometer, single-stage-quadrupol system, intensities relative to base peak. TGA: Mettler Toledo TGA/SDTA 851, heating rate: 10 °C/min, nitrogen flow: 50 mL/min. SAXS: Bruker AXS Nano-STAR equipped with a HI-STAR area detector. Potentiometric titrations: Schott Instruments ProLab 2000 equipped with an Ag/AgCl glass electrode. Tetrakis(μ_2-p-Hydroxybenzoato-O,O′)-bis(dimethylsulfoxide-O)-dicopper dimethylsulfoxide solvate **5** was synthesized according to literature [36].

DMF was distilled over CaH_2 in vacuum and stored over molecular sieve 4 Å prior to use. All other solvents and reagents were of reagent grades and used as received.

4.2. Dimethyl-5-(2-(2-hydroxyethoxy)ethoxy) benzene-1,3-dicarboxylic acid (*1*)

Under argon, a suspension of 10 g (47.6 mmol) dimethyl-5-hydroxy-1,3-benzenedicarboxylic acid, 13.4 g (80.9 mmol) potassium iodide, 7.1 g (57.1 mmol) potassium carbonate and 17.8 g (142.8 mmol) 2-(2-chloroethoxy)ethanol in 500 mL acetonitril was refluxed for 24 h. The solvent was evaporated after filtration and 1000 mL 1 M HCl were added to the residue. The aqueous phase was extracted ethyl acetate, and the combined organic phases were washed with 100 mL brine and dried over sodium sulfate. The solvent was evaporated, and the crude product was subjected to chromatography (silica, ethyl acetate:cyclohexane 2:1) to give **1** (11 g, 79%) as a white powder mp 59.0–61.3 °C. *Anal.* Calc. $C_{14}H_{18}O_7$: C, 56.4; H, 6.1. Found: C, 56.3; H, 6.1%. ν_{max}(KBr)/cm^{-1} 3300, 2958, 2925, 2883, 1726, 1595, 1461, 1435, 1347, 1310, 1244, 1133, 1051, 997, 874, 756, 719, 668, 616, 590, 549 and 458; δ_H(400 MHz; DMSO-d_6) 8.25 (1 H, t, $J_{1,4}$ 1.3, Aryl), 7.76 (2 H, d, $J_{1,4}$ 1.3, Aryl), 4.21 (2 H, dd, $J_{1,3}$ 5.4, $J_{1,3}$ 3.7, CH_2), 3.91 (6 H, s, OCH_3), 3.87 (2 H, dd, $J_{1,3}$ 5.4, $J_{1,3}$ 3.7, CH_2), 3.75 (2 H, dd, $J_{1,3}$ 5.4, $J_{1,3}$ 3.7, CH_2), 3.66 (2 H, dd, $J_{1,3}$ 5.4, $J_{1,3}$ 3.7, CH_2) and 2.33 (1 H,br s, OH); δ_C(100 MHz; DMSO-d_6) 166.1, 158.8, 131.7, 123.2, 120.0, 72.7, 69.5, 68.0, 61.8 and 52.5; *m/z* (CI) 565 (2M-CH_3O^-, 100%), 299 (M+H^+, 18%)and 267 (M-CH_3O^-, 39).

4.3. 5-(2-(2-Hydroxyethoxy)ethoxy)benzene-1,3-dicarboxylic acid (*2*)

10 g (33.6 mmol) dimethyl-5-(2-(2-hydroxyethoxy)ethoxy)benzene-1,3-dicarboxylic acid **1** and 11.3 g (201 mmol) potas-

sium hydroxide were dissolved in 200 mL ethanol: water (1:1) and refluxed for 6 h. The solvent was evaporated, the residue was dissolved in 50 mL water and adjusted with 1 M HCl to pH 1–2. The aqueous phase was extracted ethyl acetate, and the combined organic phases were washed with 100 mL brine and dried over sodium sulfate. The solvent was evaporated to give **2** (8.8 g, 97%) as a white powder mp 173.5–175.2 °C. *Anal.* Calc. for $C_{12}H_{14}O_7$: C, 53.3; H, 5.2. Found: C, 56.4; H, 5.4%. ν_{max}(KBr)/cm^{-1} 3186, 2937, 2620, 1725, 1698, 1612, 1457, 1438, 1394, 1286, 1191, 1128, 1063, 981, 933, 886, 861, 798, 734, 633, 588, 543, 508 and 450; δ_H(400 MHz; DMSO-d_6) 13.3 (2 H, s, COOH), 8.08 (1 H, t, $J_{1,4}$ 1.3, Aryl), 7.65 (2 H, d, $J_{1,4}$ 1.3, Aryl), 4.65 (1 H, br s, OH), 4.21 (2 H, t, $J_{1,3}$ 4.4, CH_2), 3.77 (2 H, t, $J_{1,3}$ 4.4, CH_2) and 3.45-3.55 (4 H, m, CH_2); δ_C(100 MHz; DMSO-d_6) 166.9, 159.1, 133.1, 122.8, 119.5, 72.9, 69.2, 68.3 and 60.7; *m/z* (CI) 253 (M-OH$^-$, 100%).

4.4. Tetracosakis(μ4-5-(2-(2-hydroxyethoxy)ethoxy)benzene-1,3-dicarboxylato)-tetracosa-copper(II) methanol solvate (3)

0.9 mL (7.4 mmol) 2,6-dimethylpyridine were added to a solution of 0.9 g (3.7 mmol) $Cu(NO_3)_2{\cdot}3H_2O$ and 1.0 g (3.7 mmol) **2** in 100 mL methanol within 1 min under vigorous stirring. The immediately formed blue suspension was stirred for 30 min, filtered and washed four times with 100 mL methanol, dried over night in air and afterwards in vacuum at room temperature to give **3** (1.2 g, 95%) as a blue powder. *Anal.* Calc. for $[Cu_{24}(C_{12}H_{12}O_7)(CH_3OH)_{24}]$: C, 42.9; H, 4.4. Found: C, 42.8; H, 4.5%. ν_{max}(KBr)/cm^{-1} 3382, 2926, 2860, 1636, 1589, 1457, 1380, 1267, 1126, 1056, 884, 774, 731 and 492.

4.5. Tetracosakis(μ4-5-(2-(2-hydroxyethoxy)ethoxy)benzene-1,3-dicarboxylato)-dodecaaqua-hexakis(dimethylsulfoxid)-hexamethanol tetracosa-copper(II) (3b)

Green single crystals of **3b** were recrystallised by vapour diffusion of *n*-butanol into a solution of **3** in DMSO, mounted in inert oil and transferred to the cold gas stream of the diffractometer.

4.6. μ5-5-(2-(2-Hydroxyethoxy)ethoxy)benzene-1,3-dicarboxylato)-hemiaqua-tetracosa-copper(II)N,N-dimethylformamide solvate (4)

12 mg (33 μmol) of **3** and (32.4 mg, 120 μmol) of **2** were dissolved in 3 mL of H_2O:DMF (1:1) and left undisturbed at room temperature for 8 weeks to obtain **4** (10.9 mg, 90%) as blue crystals which were transferred into inert oil and transferred to the cold gas stream of the diffractometer. *Anal.* Calc. for $[Cu_2(C_{12}H_{12}O_7)_2(H_2O)]{\cdot}(C_3H_7NO)$: C, 43.0; H, 4.4; N, 1.9. Found: C, 41.8; H, 4.9; N, 2.4%. ν_{max}(KBr)/cm^{-1} 3422, 2932, 2863, 1634, 1590, 1458, 1418, 1378, 1322, 1271, 1124, 1066, 892, 775, 927 and 492.

4.7. Crystal structure determination of 3b and 4

Intensity data for **3b** and **4** were collected at 153 K on a STOE-IPDS image-plate diffractometer (graphite monochromator) using Mo Kα radiation (λ = 0.7107 Å). The data were corrected for Lorentz and polarisation effects, and multi-scan absorption correction [37] was applied for **4**. Programs used: data collection: Bruker XSCANS [38], data reduction: Bruker SHELXTL [39], structure solution: SHELXS-97 [40], structure refinement: SHELXL-97 [41], molecular graphics: Diamond V3.1. [42], Mercury V1.5 [43]. Structures were solved using direct methods and refined by full-matrix least squares on $|F|^2$. All disordered atoms and atoms with non-positive U_{eq} were calculated with isotropic, all others with anisotropic displacement parameters. Hydrogen atoms were placed in geometrically calculated positions. For **3b**, an exact determination of the total amount and identity of the non-coordinated solvent molecules is not possible due to their strong disorder. Due to weak scattering of the crystals of **3b**, reflexes above 15° Θ were omitted from the structure solution and all side chain atoms were refined isotropically, and certain atom distances were specified as fixed due to problems caused by the diffuse electron density of the disordered solvent, guest molecules and 2-(2-hydroxyethoxy)ethoxy groups. Details for crystal data collection and final refinement parameters of **3b** and **4** are summarized in Tables 2 and 3. See Supplementary Material for details.

4.8. Determination of equilibrium constants

Spectra were recorded on a J&M TIDAS equipped with 1 cm quartz cuvettes at 25.0 (**2**) °C in the range of 500–1100 nm, the ionic strength was fixed at 0.5 M using KNO_3. Studies were carried out using a precision piston microburet (Eppendorf) to add the copper(II) carboxylates to 2 mL of solvent (H_2O:DMF 1:1). Between 18 and 25 solutions were prepared with a $[CuL]_{tot}$ concentration ranging between 0.0004 and 0.05 mol/L. For **3**, a fixed ratio of $[HOAc]/[CuL]_{tot}$ = 2 was used to facilitate the dissociation of the complexes, whereas copper(II) acetate and copper(II) 4-hydroxy-

Table 2
Crystallographic data for **3b**.

Formula	$C_{306}H_{372}Cu_{24}O_{192}S_6$
Formula weight	8839.65
Crystal colour, habit	green, block
Crystal dimensions (mm)	0.31 × 0.31 × 0.27
Crystal system	cubic
Space group	$Pa\bar{3}$ (#205)
a (Å)	38.119(4)
V (Å^3)	55387(11)
Z	4
D_{calc} (g cm^{-3})	1.060
F(0 0 0)	18144
μ (mm^{-1})	0.993
Number of observations (all reflections)	38537
R^a [$I > 2\sigma(I)$]	0.1004
R^b (all reflections)	0.2910
Goodness-of-fit (GOF)	0.745
$\Delta\rho_{max}$ and $\Delta\rho_{min}$ (e Å^{-3})	0.290 and −0.213

GOF = $[\sum w(F_o^2 - F_c^2)^2/(N_o - N_v)]^{1/2}$.
[a] $R = \sum ||F_o| - |F_c|| / \sum |F_o|$.
[b] $wR = [\sum(w(F_o^2 - F_c^2)^2) / \sum w(F_o^2)^2]^{1/2}$.

Table 3
Crystallographic data for **4**.

Formula	$C_{27}H_{33}Cu_2NO_{16}$
Formula weight	754.64
Crystal colour, habit	green, plate
Crystal dimensions (mm)	0.08 × 0.39 × 0.46
Crystal system	orthorhombic
Space group	$P2_12_12$ (#18)
a (Å)	18.253(4)
b (Å)	18.660(4)
c (Å)	11.928(2)
V (Å^3)	4062.6(14)
Z	4
D_{calc} (g cm^{-3})	1.234
F(0 0 0)	1552
μ (mm^{-1})	1.106
Number of observations (all reflections)	32129
R^a [$I > 2\sigma(I)$]	0.1227
R^b (all reflections)	0.3017
Goodness-of-fit (GOF)	1.295
$\Delta\rho_{max}$ and $\Delta\rho_{min}$ (e Å^{-3})	2.015 and −1.316

GOF = $[\sum w(F_o^2 - F_c^2)^2/(N_o - N_v)]^{1/2}$.
[a] $R = \sum ||F_o| - |F_c|| / \sum |F_o|$.
[b] $wR = [\sum(w(F_o^2 - F_c^2)^2) / \sum w(F_o^2)^2]^{1/2}$.

benzoate were measured with a constant concentration of 0.140 mol/L acetic acid or 4-hydroxybenzoic acid, respectively. For **3**, the spectra were measured after 6 months to ensure complete equilibration. Equilibrium constants were calculated in a similar way as already described for copper acetate [11a] using Gauss–Newton non-linear least square fitting (See Supplementary Material).

4.9. Small-angle X-ray scattering (SAXS)

Compound **3** was dissolved in DMF at a concentration of 18 g/L. The solutions were filtered using 0.2 μm pore-size filters. The scattering experiments were done with a Bruker AXS Nano-STAR equipped with a HI-STAR area detector. The light source was a conventional X-ray tube operating at 35 mA and 40 kV (Cu Kα = 0.154 nm). The blank-scattering contributions of the solvent, sample holder, and incoherent scattering were subtracted prior to any calculations. The scattering data were transformed into pair-distance distribution functions (PDDF) via the program GNOM [28]. X-ray solution scattering from the atomic coordinates of **3b** was evaluated with the program CRYSOL [31]. The program DAMMIN [29] was used for ab initio shape determination from the PDDF (by simulated annealing using a single phase dummy atom model).

Acknowledgement

The authors are grateful to the Landesgraduiertenförderung Baden-Württemberg for financial support.

Appendix A. Supplementary material

CCDC 766959 and 766958 contains the supplementary crystallographic data for **3b** and **4**. These data can be obtained free of charge from The Cambridge Crystallographic Data Centre via www.ccdc.cam.ac.uk/data_request/cif.

Supplementary data associated with this article can be found, in the online version, at doi:10.1016/j.ica.2010.06.022.

References

[1] (a) A. Ziv, A. Grego, S. Kopilevich, L. Zeiri, P. Miro, C. Bo, A. Müller, I.A. Weinstock, J. Am. Chem. Soc. 131 (2009) 6380–6382;
(b) A. Müller, S. Sarkar, S.Q. Shah, H. Bögge, M. Schmidtmann, P. Kögerler, B. Hauptfleisch, A.X. Trautwein, V.V. Schünemann, Angew. Chem., Int. Ed. Engl. 38 (1999) 3238–3241;
(c) A. Müller, S.Q.N. Shah, H. Bögge, M. Schmidtmann, Nature 397 (1999) 48–50;
(d) D.J. Cram, M.E. Tanner, R. Thomas, Angew. Chem., Int. Ed. Engl. 30 (1991) 1024–1027;
(e) X. Liu, G. Chu, R.A. Moss, R.R. Sauers, R. Warmuth, Angew. Chem., Int. Ed. 44 (2005) 1994–1997;
(f) M. Ziegler, J.L. Brumaghim, K.N. Raymond, Angew. Chem., Int. Ed. 39 (2000) 4119–4121;
(g) J. Kang, J. Rebek, Nature 385 (1996) 50–52;
(h) R. Warmuth, J.-L. Kerdelhué, S. Sánchez Carrera, K.J. Langenwalter, N. Brown, Angew. Chem., Int. Ed. 41 (2002) 96–99;
(i) M. Yoshizawa, Y. Takeyama, T. Kusukawa, M. Fujita, Angew. Chem., Int. Ed. 41 (2002) 1347–1349;
(j) M. Yoshizawa, T. Kususkawa, M. Fujita, S. Sakamoto, K. Yamaguchi, J. Am. Chem. Soc. 123 (2001) 10454–10459;
(k) M. Yoshizawa, Y. Takeyama, T. Okano, M. Fujita, J. Am. Chem. Soc. 125 (2003) 3243–3247;
(l) M. Yoshizawa, S. Miyagi, M. Kawano, K. Ishiguro, M. Fujita, J. Am. Chem. Soc. 126 (2004) 9172–9173;
(m) M.L. Merlau, M.P. Mejia, S.T. Nguyen, J.T. Hupp, Angew. Chem., Int. Ed. Engl. 40 (2001) 4239–4242;
(n) M. Yoshizawa, M. Tamura, M. Fujita, Science 312 (2006) 251–254.
[2] (a) C.L.D. Gibb, B.C. Gibb, J. Am. Chem. Soc. 126 (2004) 11408–11409;
(b) S.T. Mough, J.C. Goeltz, K.T. Holman, Angew. Chem. Int. Ed. 43 (2004) 5631–5635.
[3] (a) D.B. Amabilino, J.F. Stoddart, Chem. Rev. 95 (1995) 2725–2828;
(b) D.B. Amabilino, M. Asakawa, P.R. Ashton, R. Ballardini, V. Balzani, M. Belohradsky, A. Credi, M. Higuchi, F.M. Raymo, T. Shimizu, J.F. Stoddart, M. Venturi, K. Yase, New J. Chem. 22 (1998) 959–972;
(c) Monographs in Supramolecular Chemistry: J.F. Stoddard (Ed.), Royal Society of Chemistry, vols. 1-6, Cambridge, UK, 1989, 1991, 1994–1996;
(d) F.A. Cotton, P. Lei, C. Lin, C.A. Murillo, X. Wang, S.Y. Yu, Z.X. Zhang, J. Am. Chem. Soc. 126 (2004) 1518–1525.
[4] (a) M. Tominaga, K. Suzuki, T. Murase, M. Fujita, J. Am. Chem. Soc. 127 (2005) 11950–11951;
(b) M. Tominaga, K. Suzuki, M. Kawano, T. Kusakawa, T. Ozeki, S. Sakamoto, K. Yamaguchi, M. Fujita, Angew. Chem. 116 (2004) 5739–5743;
(c) N. Takeda, K. Unemoto, K. Yamaguchi, M. Fujita, Nature 398 (1999) 794–796;
(d) B. Olenyuk, J.A. Whiteford, A. Fechtenkötter, P.J. Stang, Nature 398 (1999) 796–799;
(e) Z. Ni, A. Yassar, T. Antoun, O.M. Yaghi, J. Am. Chem. Soc. 127 (2005) 12752–12753;
(f) P. Guinan, M. McCann, H. Ryan, Polyhedron 11 (1992) 205–210;
(g) A.C. Sudik, A.R. Millward, N.W. Ockwig, A.P. Côté, J. Kim, O.M. Yaghi, J. Am. Chem. Soc. 127 (2005) 7110–7118;
(h) F.A. Cotton, C. Lin, C.A. Murillo, Inorg. Chem. 40 (2001) 6413–6417;
(i) F.A. Cotton, L.M. Daniels, C. Lin, C.A. Murillo, Chem. Commun. (1999) 841–842;
(j) S. Leininger, B. Olenyuk, P.J. Stang, Chem. Rev. 100 (2000) 853–908.
[5] (a) Y. Ke, D.J. Collins, H.-C. Zhou, Inorg. Chem. 44 (2005) 4154–4156;
(b) B. Moulton, J. Lu, A. Mondal, M.J. Zaworotko, Chem. Commun. 9 (2001) 863–864;
(c) M. Eddaoudi, J. Kim, J.B. Wachter, H.K. Chae, M. O'Keeffe, O.M. Yaghi, J. Am. Chem. Soc. 123 (2001) 4368–4369;
(d) H. Abourahma, A.W. Coleman, B. Moulton, B. Rather, P. Shahgaldian, M.J. Zaworotko, Chem. Commun. 22 (2001) 2380–2381;
(e) G.J. McManus, Z. Wang, M.J. Zaworotko, Cryst. Growth Des. 4 (2004) 11–13;
(f) H. Furukawa, J. Kim, K.E. Plass, O.M. Yaghi, J. Am. Chem. Soc. 128 (2006) 8398–8399.
[6] M. Tonigold, J. Hitzbleck, S. Bahnmüller, G. Langstein, D. Volkmer, Dalton Trans. (2009) 1363–1371.
[7] Dodecanuclear Pd(II)-based nanoballs (Pd(II)12L24) complexes are remarkably stable and the half-lives are much longer than those for comparable monodentate Pd(II)-pyridine complexes by a factor of 10^{-5} s. Once formed, the 36-component molecular spheres behave like covalent compounds: S. Sato, Y. Ishido, M. Fujita, J. Am. Chem. Soc. 131 (2009) 6064-6065.
[8] (a) J. Kang, J. Rebek, Nature 385 (1997) 50–52;
(b) E.S. Barrett, J.L. Irwin, A.J. Edwards, M.S. Sherburn, J. Am. Chem. Soc. 126 (2004) 16747–16749;
(c) J. Sherman, Chem. Commun. (2003) 1617–1623;
(d) K. Rissanen, Angew. Chem. Int. Ed. 44 (2005) 3652–3654;
(e) F. Hof, S.L. Craig, C. Nuckolls, J. Rebek Jr., Angew. Chem. Int. Ed. 41 (2002) 1488–1508;
(f) M.A. Mateos-Timoneda, M. Crego-Calama, D.N. Reinhoudt, Chem. Soc. Rev. 33 (2004) 363–372;
(g) L.R. MacGillivray, J.L. Atwood, Angew. Chem. Int. Ed. 38 (1999) 1018–1033;
(h) L.R. MacGillivray, J.L. Atwood, Nature 389 (1997) 469–472;
(i) A. Shivanyuk, J. Rebek, Chem. Commun. (2001) 2424–2425;
(j) L.J. Prins, J. Huskens, F. De Jong, P. Timmerman, D.N. Reinhoudt, Nature 398 (1999) 498–502;
(k) L.J. Prins, F. De Jong, P. Timmerman, D.N. Reinhoudt, Nature 408 (2000) 181–184;
(l) X. Liu, R. Warmuth, J. Am. Chem. Soc. 128 (2006) 14120–14127;
(m) D.J. Cram, M.E. Tanner, R. Thomas, Angew. Chem. 103 (1991) 1048–1051.
[9] (a) A. Marquis-Rigault, A. Dupont-Gervais, P.N.W. Baxter, A. Van Dorsselaer, J.-M. Lehn, Inorg. Chem. 35 (1996) 2307–2310;
(b) C. Piguet, J.C. Bünzli, G. Bernardinelli, C.G. Borchert, P. Froidevaux, J. Chem. Soc., Dalton Trans. (1995) 83–97;
(c) N. Fatin-Rouge, S. Blanc, A. Pfeil, A. Rigault, A.-M. Albrecht-Gary, J.-M. Lehn, Helv. Chim. Acta 84 (2001) 1694–1711;
(d) N. Fatin-Rouge, S. Blanc, E. Leize, A. Van Dorsselaer, P. Baret, J.-L. Pierre, A.-M. Albrecht-Gary, Inorg. Chem. 39 (2000) 5771–5778;
(e) M. Fujita, F. Ibukuro, K. Yamaguchi, K. Ogura, J. Am. Chem. Soc. 117 (1995) 4175–4176;
(f) B. Hasenkopf, J.-M. Lehn, N. Boumediene, E. Leize, A. Van Dorsselaer, Angew. Chem. Int. Ed. 37 (1998) 3265–3268.
[10] (a) J. Chen, S. Körner, S.L. Craig, D.M. Rudkevich, J. Rebek Jr., Nature 415 (2002) 385–386;
(b) E.S. Barrett, T.J. Dale, J. Rebek Jr., J. Am. Chem. Soc. 129 (2007) 8818–8824;
(c) T. Gottschalk, B. Jaun, F. Diederich, Angew. Chem. Int. Ed. 46 (2007) 260–264;
(d) T. Amaya, J. Rebek Jr., J. Am. Chem. Soc. 126 (2004) 6216–6217;
(e) L.C. Palmer, J. Rebek Jr., Org. Biomol. Chem. 2 (2004) 3051–3059;
(f) L.J. Prins, E.E. Neuteboom, V. Paraschiv, M. Crego-Calama, P. Timmerman, D.N. Reinhoudt, J. Org. Chem. 67 (2002) 4808–4820.
[11] (a) Y. Doucet, G.W. Marion, Compt. Rend. 240 (1955) 1616–1618;
(b) Y. Doucet, R. Cogniac, Compt. Rend. 240 (1955) 968–972;
(c) S.C. Sircar, S. Aditya, B. Prasad, J. Ind. Chem. Soc. 30 (1953) 633–636;
(d) J.W. Bunting, K.M. Thong, Can. J. Chem. 48 (1970) 1654–1656.
[12] R.L. Martin, A. Whitley, J. Chem. Soc. (1958) 1394–1402.
[13] R.W. Larsen, G.J. McManus, J.J. Perry IV, E. Rivera-Otero, M.J. Zaworotko, Inorg. Chem. 46 (2007) 5904–5910.
[14] C.A. Hunter, H.L. Anderson, Angew. Chem. Int. Ed. 48 (2009) 7488–7499.

[15] B. Zhang, R. Breslow, J. Am. Chem. Soc. 115 (1993) 9353–9354.
[16] P. Ballester, A.I. Oliva, A. Costa, P.M. Deyà, A. Frontera, R.M. Gomila, C.A. Hunter, J. Am. Chem. Soc. 128 (2006) 5560–5569.
[17] A. Marquis-Rigault, A. Dupont-Gervais, P.N.W. Baxter, A.V. Dorsselaer, J.-M. Lehn, Inorg. Chem. 35 (1996) 2307–2310.
[18] (a) H. Abouhrama, G.J. Bodwell, J. Lu, B. Moulton, I.R. Pottie, R.B. Walsh, M.J. Zaworotko, Cryst. Growth Des. 3 (2003) 513–519;
(b) D.-X. Xue, Y.-Y. Lin, X.-N. Cheng, X.-M. Chen, Cryst. Growth Des. 7 (2007) 1332–1336.
[19] (a) J.J. Perry, G.J. McManus, J.M. Zawarotko, Chem. Commun. 22 (2004) 2534–2535;
(b) M. Eddaoudi, J. Kim, D. Vodak, A. Sudik, J. Wachter, M. O'Keeffe, O.M. Yaghi, Proc. Natl. Acad. Sci. USA 99 (2002) 4900–4904;
(c) B. Moulton, H. Abourahma, M.W. Bradner, J. Lu, G.J. McManus, M.J. Zaworotko, Chem. Commun. 12 (2003) 1342–1343.
[20] G.F. Swiegers, J. Malefetse, Chem. Rev. 100 (2000) 3483–3537.
[21] G. Ercolani, J. Phys. Chem. B 102 (1998) 5699–5703.
[22] (a) H.L. Anderson, Inorg. Chem. 33 (1994) 972–981;
(b) X. Chi, A.J. Guerin, R.A. Haycock, C.A. Hunter, L.D. Sarson, J. Chem. Soc. Chem. Commun. (1995) 2563–2565;
(c) D.S. Lawrence, T. Jiang, M. Levett, Chem. Rev. 95 (1995) 2229–2260.
[23] (a) W. Ostwald, Z. Phys. Chem. 22 (1897) 289–330;
(b) W. Ostwald, The Fundamental Principles of Chemistry, Longmans, Green and Co., New York, NY, 1909; see also A.F. Holleman, Lehrbuch der Anorganischen Chemie, de Gruyter, Berlin, New York, NY, 1925.
[24] DMSO: N. Judas, Acta Cryst. Sect. E 61 (2005) 2217–2219;
CH_3OH:I. Bkouche-Waksman, C. Bois, G.A. Popovitch, P.L. Haridon, Bull. Soc. Chim. Fr. (1980) 69–71;
H_2O:G.M. Brown, R. Chidambaram, Acta Cryst. Sect. B 29 (1973) 2393–2403;
$ArOCH_2CH_2OH$:K. Goubitz, E.J. Sonneveld, V.V. Chernyshev, A.V. Yatsenko, S.G. Zhukov, C.A. Reiss, H. Schenk, Z. Kristallogr. 214 (1999) 469–474.
[25] A.L. Spek, J. Appl. Cryst. 36 (2003) 7–13.
[26] The van der Waals radius of C (0.17 nm) was used to calculate the width of the apertures: A. Bondi, J. Phys. Chem. 68 (1964) 441–451.
[27] O. Glatter, J. Appl. Crystallogr. 12 (1979) 166–175.
[28] (a) D.I. Svergun, J. Appl. Cryst. 24 (1991) 485–492;
(b) D.I. Svergun, J. Appl. Cryst. 25 (1991) 495–503.
[29] D.I. Svergun, Biophys. J. 76 (1999) 2879–2886.
[30] J. Lipfert, S. Doniach, Annu. Rev. Biophys. Biomol. Struct. 36 (2007) 307–327.
[31] D.I. Svergun, C. Barberato, M.H.J. Koch, J. Appl. Cryst. 28 (1995) 768–773.
[32] (a) L. Dubicki, Aust. J. Chem. 25 (1972) 1141–1149;
(b) G.W. Reimann, G.F. Kokoszka, G. Gordon, Inorg. Chem. 4 (1965) 1082–1084;
(c) L. Dubicki, R.L. Martin, Inorg. Chem. 5 (1966) 2203–2209;
(d) D.S. McClure, J. Chem. Phys. 39 (1963) 2850–2855.
[33] (a) C. Tanford, J. Phys. Chem. 78 (1974) 2469–2479 (and references cited herein);
[b] Y. Moroi, Micelles: Theoretical and Applied Aspects, Springer-Verlag, Berlin, 1992, pp. 56-63 (and references cited herein)
[34] [a] A.E. Martell, in: W. Schneider, G. Anderegg, R. Gut (Eds.), Essays in Coordination Chemistry, Berkhauser Verlag, Basel, 1964, pp. 52–64;
[b] A.W. Adamson, J. Am. Chem. Soc. 76 (1954) 1578–1579;
[c] G. Schwarzenbach, Helv. Chim. Acta 35 (1952) 2344–2359;
[d] K.B. Yatsimirskii, Theor. Exp. Chem. 16 (1980) 34–40;
[e] R.D. Hancock, A.E. Martell, Comments Inorg. Chem. 6 (1988) 237–284.
[35] Recent reviews highlighting different aspects of MOF applications: [a] M. Eddaoudi, D.B. Moler, H. Li, B. Chen, T.M. Reineke, M. O'Keeffe, O.M. Yaghi, Acc. Chem. Res. 34 (2001) 319–330;
[b] G. Férey, C. Mellot-Draznieks, C. Serre, F. Millange, Acc. Chem. Res. 38 (2005) 217–225;
[c] U. Müller, M. Schubert, F. Teich, H. Puetter, K. Schierle-Arndt, J. Pastré, J. Mater. Chem. 16 (2006) 626–636.
[36] I. Bkouche-Waksman, C. Bois, G.A. Popovitch, P. L'Haridon, Bull. Soc. Chim. Fr. 1 (1980) 69–75.
[37] R.H. Blessing, Acta Cryst. A51 (1995) 33–38.
[38] Bruker, XSCANS, Version 2.2, Bruker Analytical X-ray Systems Inc., Madison, WI, 1996.
[39] SHELXTL V6.12 2000 Bruker Analytical X-Ray Systems, Madison, WI.
[40] G.M. Sheldrick, Acta Cryst. A46 (1990) 467–473.
[41] G.M. Sheldrick, SHELXL-97, Program for X-ray Crystal Structure Refinement, University of Göttingen, Göttingen, Germany, 1997.
[42] K. Brandenburg, H. Putz GbR, Diamond – Crystal and Molecular Structure Visualization, Crystal Impact, Postfach 1251, D-53002 Bonn.
[43] C.F. Macrae, P.R. Edgington, P. McCabe, E. Pidcock, G.P. Shields, R. Taylor, M. Towler, J. van de Streek, Mercury: visualization and analysis of crystal structures, J. Appl. Cryst. 39 (2006) 453–457.